SSRG International Journal of Electronics and Communication Engineering
ISSN: 2348-8549/ https://doi.org/10.14445/23488549/IJECE-V11I12P103

Volume 11 Issue 12, 20-31, December 2024


*Original Article*

# Bandpass Filter based on Square Shaped Double Split Ring Resonator for 5G Millimeter Wave Communication

Asari Gauravkumar Ravindra[1], Shah Milind Siddharthbhai[2]

[1]*Gujarat Technological University Ahmedabad, Gujarat, India.*
[2]*Department of Electronics and Communication Engineering, Shantilal Shah Engineering College Bhavnagar, Gujarat, India.*

[1]*Corresponding Author : gauravasari24@gmail.com*

Received: 09 October 2024 Revised: 12 November 2024 Accepted: 03 December 2024 Published: 30 December 2024

***Abstract*** *- The need for high-performance RF circuits for mm-wave is increasing due to the impending implementation of the RF wireless system at mm-wave frequency range. Compact, inexpensive, high-performing, and easily integrable bandpass filters, critical front-end components for signal selection, play an important role in mm-wave communication. This work presents a new and novel planar bandpass filter based on a square shaped double split ring resonator for three distinct substrates: FR-4, Rogers TMM4, and Rogers 5880 with a center frequency of 28GHz for n257 mm-frequency band. The project's first stage involves validating the metamaterial unit cell using the Nicholson Ross Weir technique. This technique serves to confirm the presence of negative permittivity in the split ring resonator. The bandpass filter with three distinct substrates is designed in the second section using ANSYS HFSS software. Parametric analysis is performed to optimize the size of the split ring resonator and the bandpass filter. The bandpass filter, utilizing FR-4, Rogers TMM4, and Rogers 5880 substrates, demonstrates a commendable return loss of 32dB. Nevertheless, the FR-4 and Rogers TMM4 substrates exhibit an insertion loss of 1.89dB and 1.18dB, respectively, significantly higher than the 0.49dB seen for Rogers 5880. Due to its importance in the RF transceiver, a higher insertion loss in the bandpass filter can greatly affect system performance. Therefore, filters based on thick substrates are not suited for mm-wave communication. The total bandwidth of the filter in the mm-wave frequency range is 3 GHz, while the fractional bandwidth (FBW) is 15%. The filters have dimensions of 2.5x4.6mm$^2$ for FR-4 and Rogers TMM4 substrate and 2.2x4.0mm$^2$ for Rogers 5880 substrate.*

***Keywords*** *- Square Double Split Ring Resonator, Bandpass filter, Permittivity and Permeability, S parameters, ANSYS HFSS.*

## 1. Introduction

Mobile communication is one of the areas of the communication sector developing the fastest. Radio system designers focus on higher frequencies to prevent congestion and offer the necessary data rates and throughput 1]. Future 5G broadband mobile communication networks will use the under-utilized mm-wave spectrum due to the bandwidth shortage of wireless communication. The three most important potential technologies that will improve the performance of 5G cellular networks are ultra-dense networks, massively parallel communication, and significantly increased bandwidth [2].

However, using mm-wave necessitates addressing the high frequency band propagation characteristics and channel impairments, which can be further mitigated by utilizing femtocells in conjunction with electrically steerable directional antennas with constant aperture and high gain [3-6]. Despite these limitations, the benefits of using mm-wave technology in 5G are clear.

An inevitable necessity arises for the devices and components used in 5G mm-wave communication to meet the rigorous demands and performance criteria at mm-wave frequencies. Thanks to the advancement of mm-wave transceivers, it is now feasible to achieve high-speed data transmission in wireless local area networks, home networks, and personal area networks. Bandpass filters are crucial components in modern communication systems, as they selectively choose signals at specific frequencies and play a vital role in multi-function communication systems [7]. It efficiently segregates and isolates desired signals from undesirable noise and interference, guaranteeing that only the desired frequencies are transferred or processed. Furthermore, the essential requirements for these components are that they must be inexpensive, have

low losses, be small, and be easily compatible with the components found in contemporary wireless communication systems.

Much resources and research have been dedicated to developing and presenting bandpass filters with excellent selectivity, small size, and reasonable cost, especially for the mm-wave frequencies employed in 5G communication networks. Microstrip technology, known for its cost-effectiveness and widespread availability, creates planar filters. These filters can meet the rigorous criteria of wireless systems while allowing smooth integration with planar circuits.

[8] has devised a bandpass filter utilizing microstrip technology. The filter consists of a rectangular loop resonator equipped with a stepped impedance line stub at its centre and a stub on each side on the top plane. The BPF is constructed utilizing a Rogers RT/duroid 5880 substrate, characterized by a relative dielectric constant 2.2 and a loss tangent of 0.0009. The substrate has a thickness of 0.64 mm. The filter has a centre frequency of 24.4 GHz, a return loss of 39.12dB, and an insertion loss of 0.59 dB. The proposed filter has dimensions of 11.22 × 13 mm2. The parametric analysis is conducted using HFSS. Modifying the value of L4 has a negligible impact on the centre frequency. The magnitude of S11 exhibits a significant drop, although the insertion loss of S21 remains constant. As the value of W2 increases, the centre frequency, S11, and S21 drop. Changing W3 causes a shift in the centre frequency towards higher values while simultaneously reducing the value of S11. The value of S21 remains consistent. The filter's bandwidth is 2.3 GHz, and its Fractional Bandwidth (FBW) is 9.42%.

[9] has created a bandpass filter utilizing parallel coupled lines with a centre frequency of 28GHz. The filter design calculations used various substrates, including Rogers RT/duroid 3003, FR4, Rogers RT/duroid 5880, Dupont9k7, and Rogers RT/duroid 4003. Additionally, simulations were conducted to determine the values of S11 and S21. The mix of Dupont 9k7 and silver was the most appropriate choice. Nevertheless, the process of manufacture is constrained by the need for intricate and costly setups. Ultimately, the combination of Rogers RT/duroid 4003 and copper was deemed suitable. The filter has a bandwidth of 2.8 GHz with a fractional bandwidth of 0.1%.

[10] has developed a dual-band bandpass filter (BPF) by utilizing stub loaded resonators operating at 23.92 GHz and 28.38 GHz. The filter is constructed using a Rogers RT/duroid 3010 substrate, which possesses a relative dielectric constant of 10.2 and a loss tangent of 0.0022. The substrate has a thickness of 1.28 mm. The dimensions of the filter are 1.23λg x 2.02λg. T-shaped and U-shaped resonators achieve the desired frequency ranges, whereas inverted U-shaped and E-shaped resonators suppress harmonics. By altering the lengths of the stubs, it is possible to fine-tune both the lower and upper bandwidths. The lower band has an insertion loss of 1.94dB, while the upper band has an insertion loss of 2.74 dB. The return loss is roughly 17dB for both bands. The lower band has a bandwidth of 660MHz, whereas the upper band has a bandwidth of 880MHz.

[11] has developed two bandpass filters employing microstrip-based dual-mode ring resonators and half-wavelength resonators. One filter operates at a centre frequency of 34GHz, while the other operates at a centre frequency of 40GHz. The filter uses a Rogers RT/duroid 5880 substrate with a relative dielectric constant of 2.2. The dimensions of the filter are 13.80 × 17.60 mm2. The impedance ratio determines the positioning of the transmission zeros. As the impedance ratio grows, transmission zeros are generated both below and above the centre frequency. The impedance ratio values of K1 and K2 determine the passband characteristics. Both filters have an insertion loss of approximately 2.5dB and a return loss of almost 17 dB. Both filters possess a bandwidth of around 3 GHz, with a Fractional Bandwidth (FBW) of around 18%.

[12] has developed a bandpass filter using coupled lines and two stepped impedance resonators. One of the resonators, the ring resonator, is positioned at the centre of the two parallel coupled lines on both sides of the filter. The filter is constructed utilizing a Rogers RT/duroid 5880 substrate, characterized by a relative dielectric constant of 2.2 and a thickness of 0.254. The dimensions of the filter are 20.00 × 10.00 mm2. The electrical length θ4 significantly influences the positioning of even and odd mode frequencies. As the value of θ4 grows, the resonance frequency of the odd mode does not change, but the resonant frequency of the even mode shifts towards a lower frequency. As the impedance ratio K2 grows, the frequencies of both the even and odd modes fall. The location of transmission zeros can be determined using the formulae for even and odd modes. The insertion loss is less than or equal to 0.85 dB, and the return loss is more than 17 dB. The filter has a bandwidth of roughly 2 GHz, with a Fractional Bandwidth (FBW) of around 4.2%.

[13] presented a schematic of a bandpass filter utilizing lumped components with a central frequency of 28GHz. First, a 5-pole/5th order low pass Chebyshev filter is used to develop a Bandpass filter (BPF). The outcome of this design yields a return loss of 307.70dB, an insertion loss of 0dB, and an infinite bandwidth. The second half incorporates a 3-pole/3rd order low pass Chebyshev filter truncated at the centre. This filter primarily regulates the bandwidth. The obtained outcomes include a return loss of 286.92 dB and an insertion loss of 2.89E-15dB. The filter's bandwidth is 1 GHz, and its fractional bandwidth (FBW) is 3.57%.

[14] has developed a bandpass filter utilizing a grounded centre-tapped ring resonator (CTRR) with shunt capacitive

loading in 0.13-µm (Bi)-CMOS SiGe technology. The size of the core filter is 0.03 mm2. The CTRR based technique generates two transmission poles. Modifying the transmission poles' positioning makes it possible to achieve a flexible balance between the in-band flatness and bandwidth in the passband. The insertion loss measures 2.6 dB, whereas the return loss is approximately 10 dB. The filter has a bandwidth of 30 GHz and a fractional bandwidth (FBW) of 73%.

[15] has created two distinct bandpass filters by utilizing three Broadside-Coupled Resonators (BCR) with numerous Metal–Insulator–Metal (MIM) capacitors functioning as J-inverters to construct a T-shaped network. The filters are produced using a conventional 0.13-µm (Bi)-CMOS technique. The metal layers utilized in this design exhibit an electrical conductivity of roughly 3.2x107 S/m, whereas the SiO2 substrate possesses a dielectric constant of 4.1. The size of the core filter is 0.073 mm2. The initial filter design exhibits an insertion loss of 3.9dB and a return loss of approximately 20dB, whereas the second filter design demonstrates an insertion loss of 3.1dB and a return loss of around 22 dB. The bandwidth of both filters is around 25 GHz, with a Fractional Bandwidth (FBW) of 71% for the first filter and 80% for the second filter.

[16] has created a bandpass filter with four poles and four zeros, with a high level of selectivity, low insertion loss, and a small physical size. This filter is constructed using 45-nm CMOS RF-SOI (silicon-on-insulator) technology. The silicon substrate has a dielectric constant of 4.1 and a thickness of 13.70µm. The size of the core filter is 0.07 mm2. Four transmission zeroes are formed by including multiple transmission pathways, resulting in two transmission zeroes on each side of the passband. This enhancement significantly enhances out-of-band rejection. The filter design consists of three parallel resonators and one series resonator, all of which are fourth-order lumped-element components. The filter design yields four transmission poles. Resonators 1 and 3 are the primary parallel resonators connected to the input and output ports, giving rise to the middle two poles. Resonator 2 establishes the maximum pole frequency, while resonator 4 establishes the minimum pole frequency. There exist two primary transmission pathways. The first signal path goes from resonator 1 to resonator 2 and then to resonator 3, while the second signal path goes directly through resonator 4. The transmission paths dictate the filter's bandwidth. The transmission zeros are influenced by the two auxiliary routes, which are created through the cross coupling of the resonators, one on the top side and one on the lower side. Additionally, the source-load coupling generates two transmission zeros on either side of the pass band. The insertion loss is around 1.5 dB, whereas the return loss is approximately 10 dB. The filter has a 20GHz bandwidth and a fractional bandwidth (FBW) of 66%.

[17] has developed a 4th order bandpass filter utilizing a Substrate Integrated Waveguide (SIW) filled with air. The filter utilizes both electric and magnetic coupling and is constructed with 4 layers. This design aims to decrease the insertion loss significantly compared to traditional SIWs filled with dielectric materials. Nevertheless, the AFSIW has a greater physical presence than the conventional SIW filled with dielectric material. The filter is constructed with Rogers RT/Duroid 6002 substrate, which has a relative permittivity of 2.98 and a thickness of 0.508 mm for each layer. The dimensions of the filter are 7.04x17mm2. The total structure is enclosed by the top and bottom substrates, referred to as Layers 1 and 5, respectively. Layer 2 comprises cavities C1 and C4 and the feeding lines. The conductor-backed coplanar waveguide provides power to the first transition to a Substrate Integrated Waveguide (SIW) and the second to an Air-Filled Substrate Integrated Waveguide (AFSIW). Layer 3 consists of the vertical iris. Cavities C2 and C3 are in Layer 4. Magnetic coupling is established by employing an H-plane iris, whereas electric coupling is performed using E-plane coupling windows. The insertion loss is 1dB, and the return loss is 11 dB. The filer has a 3.4 gigahertz (GHz) bandwidth and a fractional bandwidth (FBW) of 10.29%.

[18] has developed a Bandpass Filter (BPF) using Substrate Integrated Waveguide (SIW) technology. An integrated structure consisting of a stepped impedance face-to-face E-shaped defected ground structure (DGS) is produced using a regular complementary stepped-impedance resonator and two face-to-face E-shaped DGS. This structure is incorporated in the top metallic layer of the substrate integrated waveguide (SIW). The filter is constructed with Rogers RT/Duroid 5880 substrate, which possesses a relative permittivity of 2.2 and a thickness of 0.254 mm. Microstrip to substrate integrated waveguide (SIW) transitions are attached to both ends of the SIW to conduct measurements. The dimensions of the filter are 2.64λg in length and 1.04λg in width. The filter has an insertion loss of 1.7dB and a return loss of 12dB. Moreover, the two E-shaped Defected Ground Structures (DGS) are directly linked, enhancing in-band frequency performance by creating three reflection zeros within the passband and two transmission zeros in the upper rejection band. The filter has a bandwidth of 3.2 GHz, and the Fractional Bandwidth (FBW) is 8.4%.

[19] has constructed a 4-pole bandpass filter utilizing Substrate Integrated Waveguide (SIW). Semi-circular slots are implemented in the upper metal layer to optimize the coupling between the resonators using an iris. The filter is constructed with Rogers RT/Duroid 5880 substrate, which possesses a relative permittivity of 2.2 and a thickness of 0.127 mm. The dimensions of the filter are 1.2λg x 1.1λg. The presence of semicircle slots affects the frequencies fe and fm, which correspond to the resonator's virtual electric and magnetic walls. The value of fe remains constant, but fm significantly decreases, increasing the coupling coefficient.

The coupling coefficient can be fine-tuned by adjusting the width of the iris and the spacing between the slots. The insertion loss is 2dB, and the return loss is 14 dB. The filter has a bandwidth of 3.3 GHz and a Fractional Bandwidth (FBW) of 11.4%.

[20] has created a dual-band bandpass filter by using a technique called etching to create two pairs of Dumbbell-Shaped Defective Ground Structures (DB-DGS) of the same size on both the ground and top layers of the Substrate Integrated Waveguide (SIW). The etched slots on the top and bottom layers are positioned at a right angle to each other. The filter is constructed with Rogers RT/Duroid 5880 substrate, which possesses a relative permittivity of 2.2 and a thickness of 0.254mm. The dimensions of the filter are 0.82λg x 0.45λg. Microstrip to substrate integrated waveguide (SIW) transitions are attached to both ends of the SIW to conduct measurements. As the width of the SIW (Substrate Integrated Waveguide) increases, the fundamental frequency lowers. On the other hand, as the length of the SIW increases, the fundamental frequency remains constant while the second frequency varies. The bandwidth at the centre frequencies of 28GHz and 38GHz is 7GHz and 2GHz, respectively. These frequencies' Fractional Bandwidths (FBW) are 25% and 5%, respectively.

[21] has devised a bandpass filter employing arrays of MEMS ohmic contact switches and bridges from 22-24GHz. The filter comprises one low pass filter component and two high pass filter sections. The low pass filter is constructed using high impedance transmission lines, which function as an inductor and a varactor diode. Conversely, the high pass filter is constructed using tunable capacitors. The filter is constructed utilizing an alumina substrate with a thickness of 635μm. The dimensions of the filter are 3.25x0.85mm2, excluding the bias pads. The insertion loss is measured at 1.69 dB, whereas the return loss is approximately 18 dB. The filter has a fractional bandwidth of 6.5%.

[22] has developed a bandpass filter using a Low-Temperature Cofired Ceramic (LTCC) material, which combines lumped and distributed circuits. Lumped circuits enable the reduction in circuit size, while distributed circuits enhance circuit performance through the incorporation of mutual coupling. The filter is constructed with a Ferro A6-M substrate with a dielectric constant of 5.9 and a thickness of 94μm. The distributed circuit is positioned in an elevated position relative to the ground plane, whereas the lumped circuit is positioned in a lower position. This configuration makes it possible to construct both parts and utilize distinct substrate heights independently. The stop band rejection can be improved with large areas of distributed and lumped circuits as well as with small substrate heights. One can employ a Perfect Electric Conductor (PEC) or mitigate losses associated with microstrip lines to minimise insertion loss resulting from radiation, conductor, and dielectric loss. Nevertheless, there is consistently a compromise between the requirement for shrinking and achieving a high Q. The insertion loss and return loss values are 0.84dB and 14dB, respectively. By incorporating two additional dielectric layers onto the microstrip line, the insertion loss is further decreased to 0.73dB. The filter has a frequency range of 5 GHz and a fractional bandwidth of 20%.

[23] has constructed a bandpass filter by utilizing parallel open circuited coupled lines. They then produced seven identical replicas of this filter to examine each replica's centre frequency, fractional bandwidth (FBW), insertion loss, and return loss. A thin substrate is preferred to achieve low insertion loss. The filter is constructed using Rogers RO4350B substrate with a thickness of 0.254 and a dielectric constant of 3.48.

Filter replicas 4, 5, 6, and 7 exhibit frequency deviation from the centre frequency and display varying levels of insertion and return loss, potentially indicating a fault in the connections' contact with the PCB. Unlike the other replicas, the fourth filter replica exhibits a notch in the stop band. The connector's inadequate electrical contact causes this. The notch disappears during measurements when the connector is placed against the signal line. Additionally, it is noted that the reflection parameter is more susceptible to variations in connector implementation and manufacturing tolerances when compared to transmission characteristics.

[24] has devised a 3rd order bandpass filter by utilizing two hairpin resonators and a zig-zag resonator to enhance the interconnection between the two resonators. The filter is constructed using Rogers 4003C substrate with a thickness of 0.203 and a dielectric constant of 3.55. The dimensions of the filter are 14.85x15.96mm2. The microstrip lines are used to supply the filter in a tapered configuration. The insertion loss ranges from 3.5 to 4 dB, whereas the return loss is 10 dB. The filter's bandwidth is 2 gigahertz, while the Fractional Bandwidth (FBW) is 7%.

The bandpass filters [14-16] utilizing Si technology are well-suited for integrating both baseband circuitry and RF front end. However, due to the low resistivity of the Si substrate used in mm-wave circuits, the on-chip passive components have low Q-factors and experience high losses in the CMOS process. Furthermore, polysilicon is employed as the gate material in CMOS devices, exhibiting a significantly higher sheet resistance than metal. As a result, this increases gate resistance, which can subsequently reduce power gain and increase noise. Consequently, polysilicon is not particularly suitable for designing mm-wave frequency bandpass filters.

Designing bandpass filters [17-20] based on Substrate Integrated Waveguide (SIW) at high frequencies is challenging due to the difficulty in fabricating the extremely

thin magnetic coupling interfaces formed by via-holes. Consequently, utilizing this type of coupling to construct SIW filters for mm-waves is exceedingly difficult.

The bandpass filters [13] and [22], based on lumped components, as well as [21], based on MEMS, are not appropriate for mass production at mm-wave frequencies due to significant fabrication tolerances. Certain aspects of the performance may exhibit high sensitivity to process variations, such as MIM capacitors, metal width, and thickness, which are limited by design requirements.

The bandpass filters [8-12] and [23-24] are implemented using the conventional microstrip-based method. While this strategy can provide higher performance, the filters built for it tend to take up a rather substantial amount of space. One potential method for reducing area is to employ the technique of folding transmission lines. However, folding transmission lines can negatively impact the overall performance of the filter since it leads to undesired coupling.

Although a significant quantity of work has been documented in the bandpass filter design using diverse technologies, to our knowledge, not much of the work has been published utilizing a square-shaped double split ring resonator at the mm-wave band of frequency.

This study describes the construction of a new bandpass filter operating at a centre frequency of 28GHz. The filter incorporates a square-shaped double split ring resonator, which acts as a metamaterial structure. This structure is known for its small size and improved electrical properties compared to previously described filters. The S-DSRR components are positioned in an antiparallel configuration between the U-shaped filter to provide a broad pass band characteristic.

The physical characteristics of the S-DSRR, such as the length of the ring, the width of the ring, and the gap, are modified to examine the changes in frequency shift, transmission, and reflection coefficients. The parameters are optimized to further enhance the return and insertion loss while achieving a distinct cutoff before and after the pass band.

## 2. Double Split Ring Resonator

The material's magnetic permeability (μ) and electric permittivity (ε) are important characteristics that significantly impact the performance of millimetre-wave circuits. The materials are classified based on their intrinsic properties. Materials classified as double-positive exhibit the property of having both positive permittivity and permeability. According to Veselago's theory [25], when both quantities possess negative values, they are referred to as double negative materials. The materials can be categorized as negative ε (permittivity) materials with negative μ (permeability). Three decades later, Pendry's presentation of a resonant double ring [26] is regarded as the fundamental component of the inaugural metamaterial ever devised. Smith published his work in 2000 [27].

Figure 1 depicts the suggested configuration of the double square split ring resonator, while Table 1 presents a comprehensive breakdown of its dimensions. The split ring resonator is called a dual split ring resonator due to its composition of two rings, as depicted in Figure 1. Four unique characteristics characterize the ring. First, the inner and outer rings' lengths. The breadth of the inner and outer rings is the second factor. The third factor is the interring spacing, the distance between the inner and outer rings.

The fourth element is the ring gap, which is the distance between the boundaries of the square open loop. The gaps in the rings allow the SRR unit to resonate at wavelengths that exceed the diameter of the rings. The second split ring, oriented in the opposite direction from the first, concentrates the electric field and substantially reduces the resonant frequency by generating substantial capacitance in the small region between the rings [28].

Figure 2 depicts the analogous circuit for the split ring resonator, represented as an LC circuit [29]. The representation of each ring can be expressed as a solenoid, with the inductance of the ring being written as Lm. Cm refers to the capacitance generated by the separation between the rings, whereas Cgap indicates the capacitance created by the plane that separates the two rings.

Equation 1 provides the ring's inductance representation [29]

$$L_m = \frac{\mu_0 Z}{S}(P_2 + T) \quad (1)$$

where S is the ring width, $P_2$ and T are the outer and inner ring lengths, and Z is the ring gap.

Equation 2 provides the capacitance between the rings [29]

$$C_m = \frac{A\varepsilon_0\varepsilon_r S(2P_2+2T-Y)}{2Z} \quad (2)$$

Where A is the equilibrium constant, Y is the gap, and ε is the permittivity.

At last, Equation 3 shows Cgap as indicating [29]

$$C_{gap} = \frac{\varepsilon_0\varepsilon_r t}{Y} \quad (3)$$

Where t stands for the ring's thickness.

The geometrical characteristics of the square split ring resonator determine its resonant frequency given as

$$f_r \approx \frac{1}{2\pi(L_m C_m)^{1/2}} \quad (4)$$

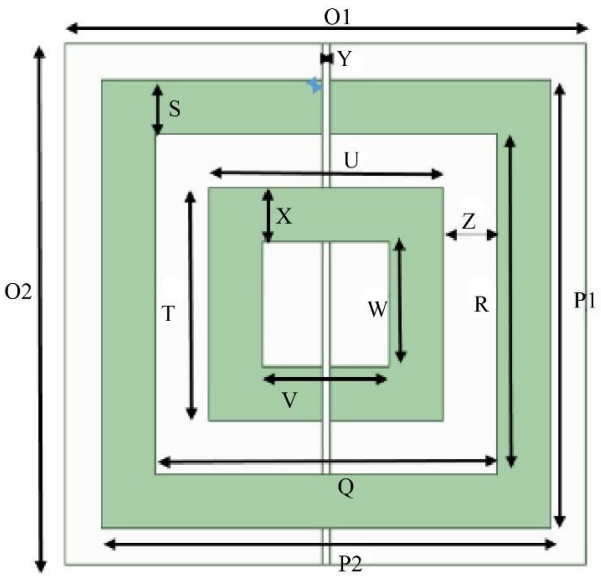


**Fig. 1 Split ring resonator**

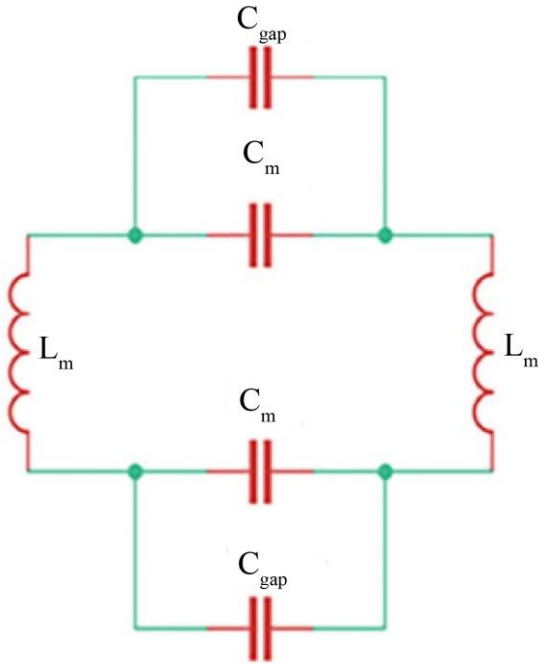


**Fig. 2 Equivalent circuit of split ring resonator [29]**

The square double split ring resonator has been designed for three distinct substrates, as outlined in Table 2. The Nicolson-Ross-Weir (NRW) method and ANSYS HFSS software are utilized to determine the permittivity, which is subsequently employed to illustrate the metamaterial characteristics of the split ring resonator depicted in Figure 1.

**Table 1. Dimensions of the double split ring resonator for three different substrates in mm units**

| Parameters | FR4 | Rogers TMM4 | Rogers 5880 |
|---|---|---|---|
| Ring Length | 0.90 | 0.90 | 1.20 |
| Ring Width | 0.13 | 0.13 | 0.15 |
| Ring Gap | 0.01 | 0.01 | 0.10 |
| Ring Spacing | 0.10 | 0.10 | 0.11 |

**Table 2. Substrate parameters of the double split ring resonator**

| Parameters | FR4 | Rogers TMM4 | Rogers 5880 |
|---|---|---|---|
| Substrate Thickness | 1.60mm | 0.63mm | 0.25mm |
| Dielectric Constant | 4.2 | 4.5 | 2.2 |
| Loss Tangent | 0.025 | 0.020 | |

Equation 5 establishes the fundamental basis for the technique. Figure 3 illustrates the effective permittivity of the double split ring resonator across several substrates employed in its design. These figures demonstrate that the resonator operates in a manner like that of a metamaterial.

$$\varepsilon_r = \frac{2}{jk_0 t}\frac{(1-V_1)}{(1+V_1)} \quad (5)$$

Where $k_0$ represents the wavenumber, while t denotes the thickness of the substrate, $V_1 = S_{11} + S_{12}$ *and* $V_2 = S_{12} - S_{11}$

Figure 4 illustrates the insertion and return losses of the split ring resonator, with the corresponding values listed in Table 3. Using a thin and low-loss substrate at the center frequency of 28GHz improves both insertion loss and return loss.

**Table 3. Insertion and Return Loss of the resonator for different substrates**

| Substrate | Insertion Loss | Return Loss |
|---|---|---|
| FR-4 | 2.42 dB | 14.62 dB |
| Rogers TMM4 | 0.75 dB | 22.80 dB |
| Rogers 5880 | 0.27 dB | 31.84 dB |

The ANSYS HFSS software is employed to do a parametric analysis of the split ring resonator, considering various lengths and widths shown in Figures 5, 6 and 7 for different substrates.

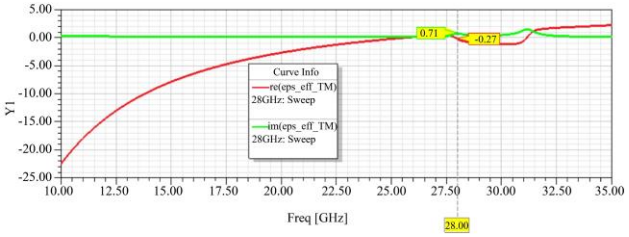


**Fig. 3(a) Effective permittivity of the S-DSRR for FR-4 substrate**

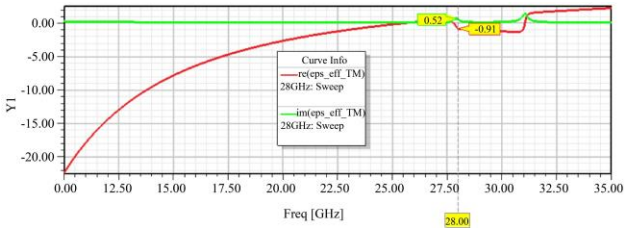


**Fig. 3(b) Effective permittivity of the S-DSRR for Rogers TMM4 substrate**

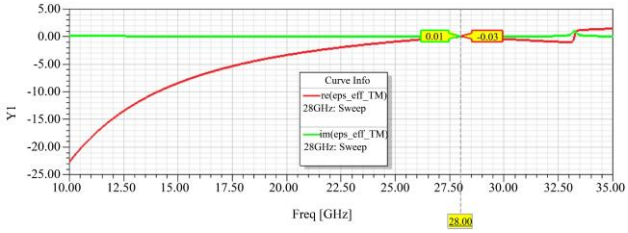


**Fig. 3(c) Effective permittivity of the S-DSRR for Rogers 5880 substrate**

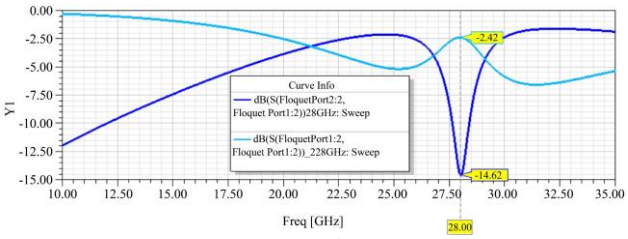


**Fig. 4(a) Insertion and Return Loss of the S-DSRR for FR-4 substrate**

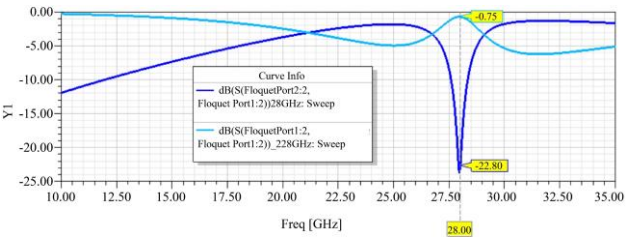


**Fig. 4(b) Insertion and Return Loss of the S-DSRR for Rogers TMM4 substrate**

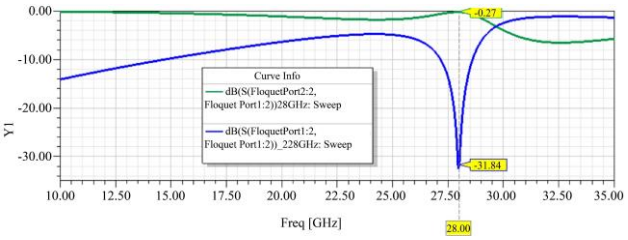


**Fig. 4(c) Insertion and Return Loss of the S-DSRR for Rogers 5880 substrate**

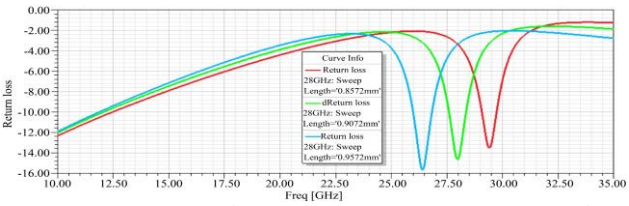


**Fig. 5(a) Return Loss of the S-DSRR based on FR-4 substrate for different lengths**

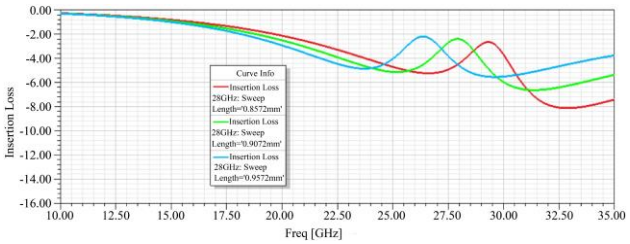


**Fig. 5(b) Insertion Loss of the S-DSRR based on FR-4 substrate for different lengths**

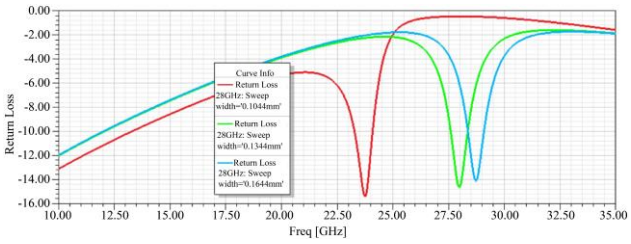


**Fig. 5(c) Return Loss of the S-DSRR based on FR-4 substrate for different widths**

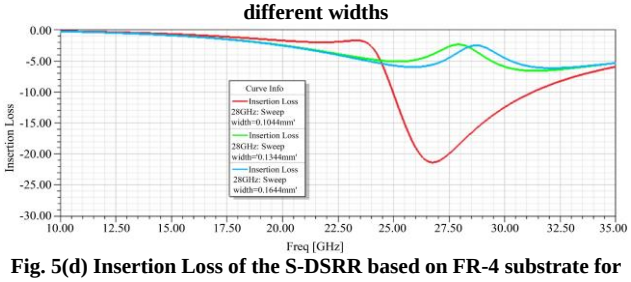


**Fig. 5(d) Insertion Loss of the S-DSRR based on FR-4 substrate for different widths**

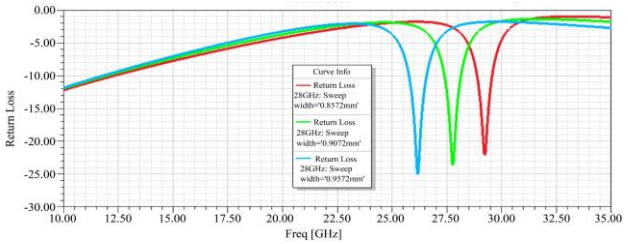


**Fig. 6(a) Return Loss of the S-DSRR based on Rogers TMM4 substrate for different lengths**

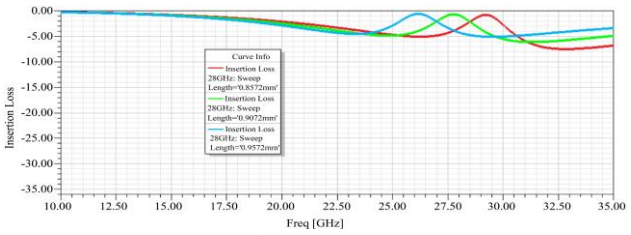


**Fig. 6(b) Insertion Loss of the S-DSRR based on Rogers TMM4 substrate for different lengths**

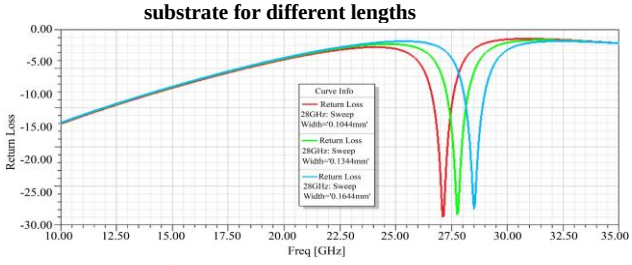


**Fig. 6(c) Return Loss of the S-DSRR based on Rogers TMM4 substrate for different widths**

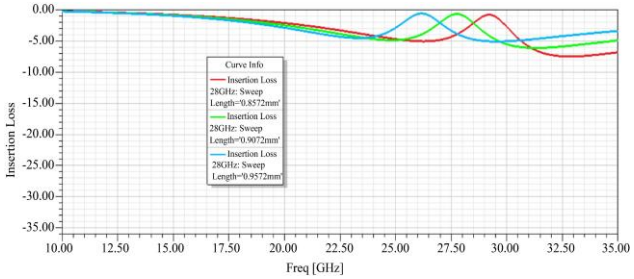


**Fig. 6(d) Insertion Loss of the S-DSRR based on Rogers TMM4 substrate for different widths**

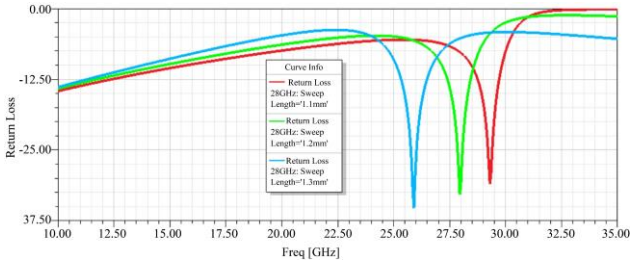


**Fig. 7(a) Return Loss of the S-DSRR based on Rogers 5880 substrate for different lengths**

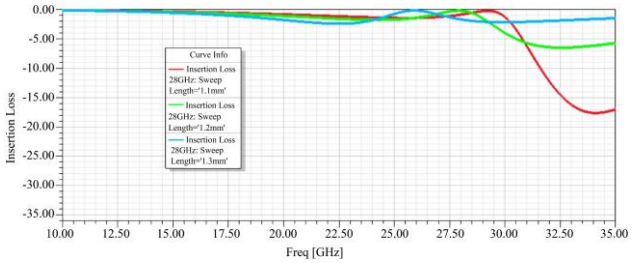


**Fig. 7(b) Insertion Loss of the S-DSRR based on Rogers 5880 substrate for different lengths**

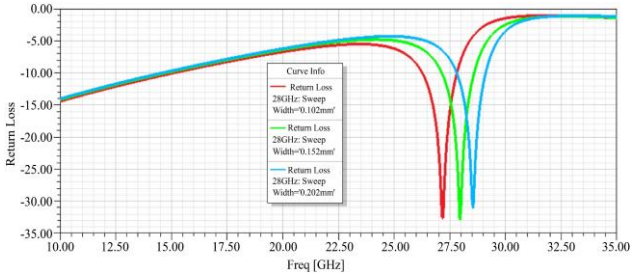


**Fig. 7(c) Return Loss of the S-DSRR based on Rogers 5880 substrate for different widths**

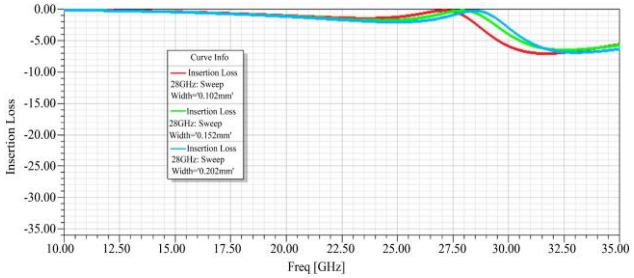


**Fig. 7(d) Insertion Loss of the S-DSRR based on Rogers 5880 substrate for different widths**

Based on the parametric analysis, it is evident that decreasing the length and width results in a shift of the center frequency towards lower frequencies. Conversely, increasing the length and breadth causes the center frequency to shift towards higher frequencies for all three substrates.

When the length and width reduce, the return loss increases and the insertion loss decreases. Conversely, the return loss drops when the length and width grow, and the insertion loss increases for all three substrates utilized.

There is no alteration in the frequency shift as the electric permittivity value lowers successively from 4.5 to 4.2 and subsequently to 2.2. Nevertheless, the return loss exhibits an upward trend, whereas the insertion loss shows a downward trend.

## 3. Proposed Bandpass Filter Design

The process of creating a band pass filter is separated into four components.

Once the appropriate substrate with the desired thickness, permittivity, and loss tangent has been chosen, as depicted in stage 1 of Figure 8(a), a cross-shaped slit is created on the ground plane.

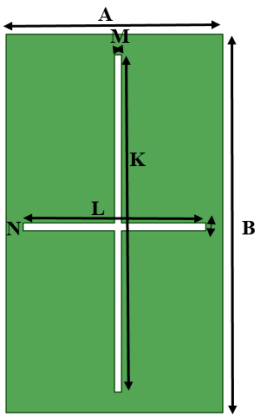


**Fig. 8 (a) Stage-1 of the bandpass filter design**

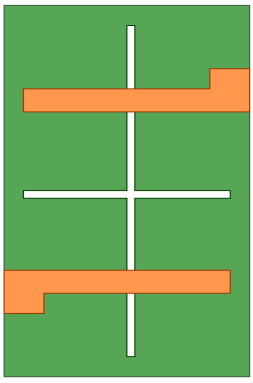

**Fig. 8 (b) Stage-2 of the bandpass filter design**

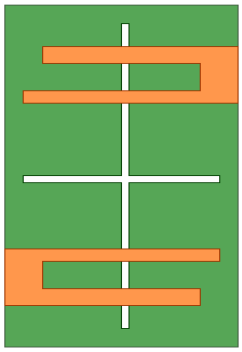

**Fig. 8 (c) Stage-3 of the bandpass filter design**

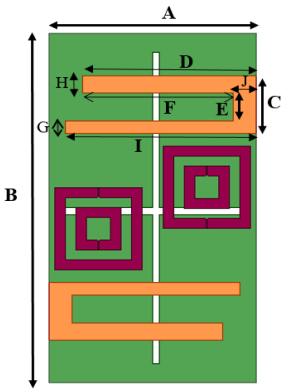


**Fig. 8 (d) Stage-4 of the bandpass filter design**

The opening, shaped like a cross, is known as the defective ground structure. Etching in the ground plane beneath the microstrip line alters the microstrip line's effective capacitance and inductance by raising the slots' resistance, capacitance, and inductance[30].

The second stage involves the construction of a microstrip feed line in the shape of an "L" with an impedance of 50 Ω. Figure 8(b) displays this as stage 2. Stage 3 in Figure 8(c) represents the development of a U-shaped filter.

In the last stage, two square split ring resonators, functioning as metamaterial, are added. These resonators are positioned 1.2 mm apart, as depicted in stage 4 of Figure 8(d).

Table 4 presents the precise measurements of the filter.

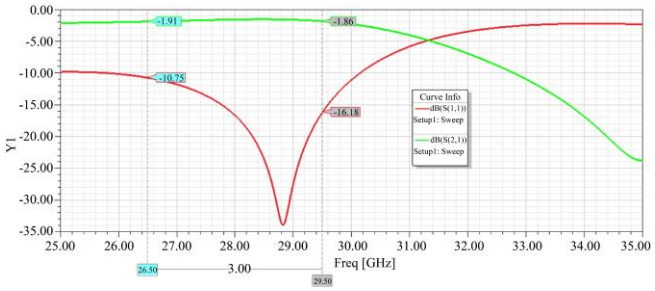


**Fig. 9(a) Frequency response of the proposed bandpass filter designed using FR-4 substrate**

**Table 4. Dimensions of the proposed bandpass filter in mm units**

| Parameter Symbol | FR4 | Rogers TMM4 | Rogers 5880 |
|---|---|---|---|
| A | 2.59 | 2.59 | 2.24 |
| B | 4.66 | 4.66 | 4.02 |
| C | 0.74 | 0.74 | 0.64 |
| D | 2.20 | 2.20 | 1.90 |
| E | 0.37 | 0.37 | 0.32 |
| F | 1.91 | 1.91 | 1.65 |
| G | 0.15 | 0.15 | 0.13 |
| H | 0.22 | 0.22 | 0.19 |
| I | 2.42 | 2.42 | 2.09 |
| J | 0.28 | 0.28 | 0.24 |
| K | 4.15 | 4.15 | 3.59 |
| L | 2.20 | 2.20 | 1.90 |
| M | 0.08 | 0.08 | 0.07 |
| N | 0.10 | 0.10 | 0.08 |

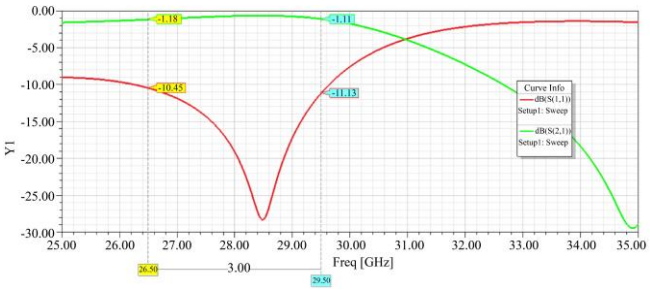


**Fig. 9(b) Frequency response of the proposed bandpass filter designed using Rogers TMM4 substrate**

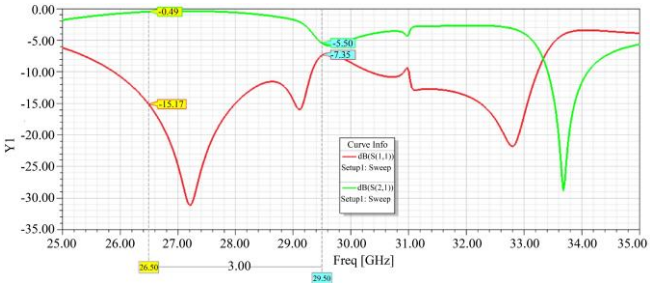


**Fig. 9(c) Frequency response of the proposed bandpass filter designed using Rogers 5880 substrate**

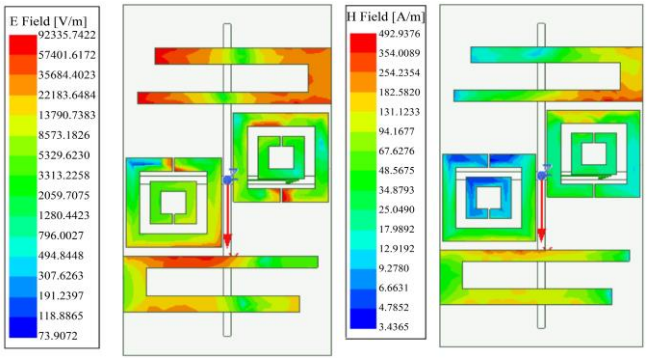


**Fig. 10(a) E and H field distribution of the proposed bandpass filter designed using FR4 substrate**

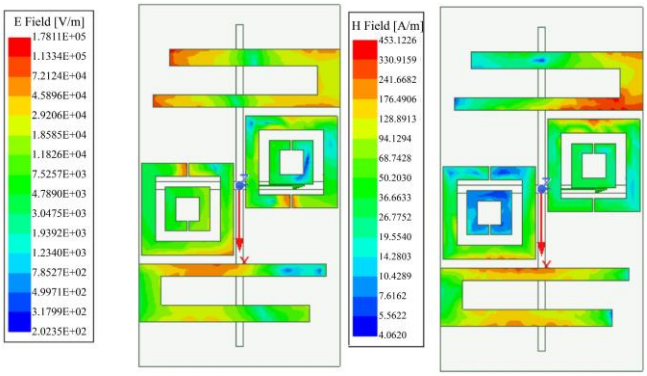


**Fig. 10(b) E and H field distribution of the proposed bandpass filter designed using Rogers TMM4 substrate**

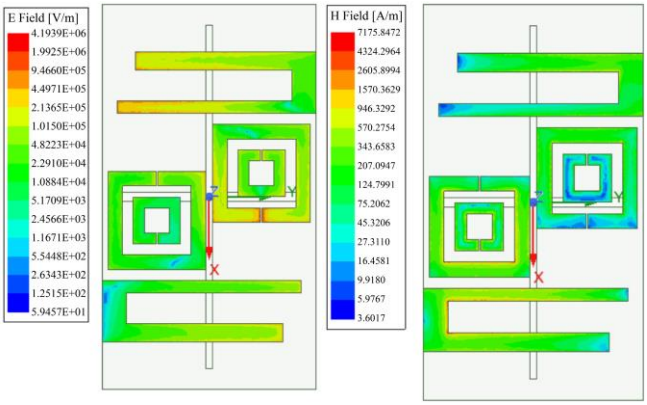


**Fig. 10(c) E and H field distribution of the proposed bandpass filter designed using Rogers 5880 substrate**

**Table 5. Insertion loss, return loss, and size of the of the proposed bandpass filter for different substrates**

| Substrate | Insertion Loss | Return Loss | Size ($mm^2$) |
|---|---|---|---|
| FR-4 | 1.91 dB | 34dB | 2.5x4.6 |
| Rogers TMM4 | 1.18 dB | 29dB | 2.5x4.6 |
| Rogers 5880 | 0.49 dB | 31dB | 2.2x4.0 |

## 4. Results

The bandpass filter, depicted in Figure 9, consists of two S-DSRR components simulated using ANSYS HFSS software and demonstrates exceptional pass band characteristics from 26.50 GHz to 29.50 GHz. The filter has a bandwidth of 3 GHz and achieves a maximum insertion loss of 1.91dB for the FR-4 substrate, 1.18dB for the Rogers TMM4 substrate, and 0.49dB for the Rogers 5880 substrate within the pass band. The results also indicate a low return loss, suggesting excellent transmission quality throughout the frequency range. 15% is the Fractional Bandwidth (FBW). According to the findings, there was a significant cutoff both before and after the pass band.

The findings are outlined in Table 5, demonstrating that decreasing the substrate's thickness and enhancing the substrate's loss tangent improve the insertion loss. The suggested band pass filter dimensions are 2.5x4.6mm2 for the FR-4 substrate and 2.2x4.0mm2 for the Rogers TMM4 substrate. These dimensions are the smallest documented in the existing literature.

The bandpass filter under consideration is analysed for its electromagnetic properties using the ANSYS HFSS program. The parameters under investigation are the electric field (V/m) and magnetic field strength (A/m). Figure 10 illustrates the analysis of the simulation results, demonstrating the transmission of radio frequency power from the input port to the output port through the bandpass filter. The illustration illustrates that the electric and magnetic field intensities primarily focus on the ring and decrease in the substrate.

## 5. Conclusion

The work commences with analysing a double split ring resonator that is part of the metamaterial family. The resonator is investigated regarding substrates possessing varying electric permittivity, thickness, and loss tangent. An inquiry is carried out to examine the permittivity, reflection, and transmission coefficients of the metamaterial unit cell.

The ANSYS HFSS program is utilized to develop and optimize a compact bandpass filter incorporating a double split ring resonator. The filter design exhibits exceptional electrical performance. The return loss at the centre frequency of 28GHz is measured to be 34dB, 29dB, and 31dB for FR-4 substrate, Rogers TMM4 substrate, and Rogers 5880 substrate, accordingly. On the other hand, the insertion loss is found to be 1.91dB, 1.18dB, and 0.49dB for the same substrates in the same order. The filter features a broad pass band with a Fractional Bandwidth (FBW) of 15%. An increased insertion loss in the bandpass filter could cause a significant impact on the overall performance of the system. Hence, filters based on thick substrates are unsuitable for mm-wave communication.

An electromagnetic field analysis was conducted using Finite Element Analysis (FEA) to study the proposed bandpass filter. The investigation revealed the transfer of power between the ports.

## References

[1] Jeffrey G. Andrews et al., "What will 5G be?," *IEEE Journal on Selected Areas in Communications*, vol. 32, no. 6, pp. 1065-1082, 2014. [CrossRef] [Google Scholar] [Publisher Link]

[2] Theodore S. Rappaport et al., "Millimeter Wave Mobile Communications for 5G Cellular: It Will Work!," *IEEE Access*, vol. 1, pp. 335-349, 2013. [CrossRef] [Google Scholar] [Publisher Link]

[3] A. Gupta, and R.K. Jha, "A Survey of 5G Network: Architecture and Emerging Technologies," *IEEE Access*, vol. 3, pp. 1206-1232, 2015. [CrossRef] [Google Scholar] [Publisher Link]

[4] A. Lee Swindlehurst et al., "Millimeter-Wave Massive MIMO: The Next Wireless Revolution?," *IEEE Communications Magazine*, vol. 52, no. 9, pp. 56-62, 2014. [CrossRef] [Google Scholar] [Publisher Link]

[5] Yong Niu et al., "A Survey of Millimeter Wave Communications (mmWave) for 5G: Opportunities and Challenges," *Wireless Networks*, vol. 21, pp. 2657-2676, 2015. [CrossRef] [Google Scholar] [Publisher Link]

[6] Tianyang Bai, Ahmed Alkhateeb, and Robert W. Heath, "Coverage and Capacity of Millimeter-Wave Cellular Networks," *IEEE Communications Magazine*, vol. 52, no. 9, pp. 70-77, 2014. [CrossRef] [Google Scholar] [Publisher Link]

[7] Zahid A. Bhat et al., "A New Method of Isolation Enhancement of Dual Band Band-Pass Filter Using Composite Mode Co-Planar Waveguide Structure for 5G and Body Centric Applications," *Iranian Journal of Science and Technology - Transactions of Electrical Engineering*, vol. 47, pp. 317-326, 2023. [CrossRef] [Google Scholar] [Publisher Link]

[8] F. Kiouach, B. Aghoutane, and M. El Ghzaoui, "Novel Microstrip Bandpass Filter for 5G mm-Wave Wireless Communications," *E-Prime - Advances in Electrical Engineering, Electronics and Energy*, vol. 6, pp. 1-6, 2023. [CrossRef] [Google Scholar] [Publisher Link]

[9] Chinmay B. Khedekar, Deeplaxmi V. Niture, and Vinay S. Kulkarni, "Designing a Microstrip Band Pass Filter for 5G Applications," *2022 International Conference on Industry 4.0 Technology (I4Tech)*, Pune, India, pp. 1-6, 2022. [CrossRef] [Google Scholar] [Publisher Link]

[10] Thierno Amadou Mouctar Balde, Franklin Manene, and Franck Moukanda Mbango, "A Dualband Bandpass Filter with Tunable Bandwidths for Automotive Radar and 5G Millimeter-Wave Applications," *Indonesian Journal of Electrical Engineering and Computer Science*, vol. 27, no. 1, pp. 309-317, 2022. [CrossRef] [Google Scholar] [Publisher Link]

[11] Amjad Altaf et al., "Design of Millimeter-Wave Microstrip BPF using Dual-Mode Ring Resonator and Folded Half-Wavelength Resonators," *2020 17th International Bhurban Conference on Applied Sciences and Technology (IBCAST)*, Islamabad, Pakistan, pp. 653-657, 2020. [CrossRef] [Google Scholar] [Publisher Link]

[12] Zahid A. Bhat et al., "Compact and Novel Coupled Line Microstrip Bandpass Filter based on Stepped Impedance Resonators for Millimetre-Wave Communications," *Frequenz*, vol. 75, no. 5-6, pp. 147-152, 2021. [CrossRef] [Google Scholar] [Publisher Link]

[13] Muhammad Rendra Perdana Kusuma Djaka, and Gunawan Wibisono, "Design of a 28 GHz Bandpass Filter for 5G Applications," *E-Komtek (Electro-Computer-Engineering) Journal*, vol. 7, no. 2, pp. 258-265, 2023. [CrossRef] [Google Scholar] [Publisher Link]

[14] Yang Yang et al., "Compact On-Chip Bandpass Filter with Improved In-Band Flatness and Stopband Attenuation in 0.13-μ (Bi)-CMOS Technology," *IEEE Electron Device Letters*, vol. 38, no. 10, pp. 1359-1362, 2017. [CrossRef] [Google Scholar] [Publisher Link]

[15] He Zhu et al., "Design of Wideband Third-Order Bandpass Filters Using Broadside-Coupled Resonators in 0.13-μm (Bi)-CMOS Technology," *IEEE Transactions on Microwave Theory and Techniques*, vol. 66, no. 12, pp. 5593-5604, 2018. [CrossRef] [Google Scholar] [Publisher Link]

[16] Li Gao, and Gabriel M. Rebeiz, "Wideband Bandpass Filter for 5G Millimeter- Wave Application in 45-nm CMOS Silicon-on-Insulator," *IEEE Electron Device Letters*, vol. 42, no. 8, pp. 1244-1247, 2021. [CrossRef] [Google Scholar] [Publisher Link]

[17] F. Parment et al., "Ka-Band Compact and High-Performance Bandpass Filter based on Multilayer Air-Filled SIW," *Electronics Letters*, vol. 53, no. 7, pp. 486-488, 2017. [CrossRef] [Google Scholar] [Publisher Link]

[18] Jian Li et al., "38-GHz SIW Filter Based on the Stepped-Impedance Face-to-Face E-Shaped DGSs for 5G Application," *Microwave and Optical Technology Letters*, vol. 61, no. 6, pp. 1500-1504, 2019. [CrossRef] [Google Scholar] [Publisher Link]

[19] Songyuan Yang et al., "Substrate Integrated Waveguide Filter based on Novel Coupling Enhanced Semicircle Slots for 5G Applications," *IEICE Electronics Express*, vol. 16, no. 8, pp. 1-4, 2019. [CrossRef] [Google Scholar] [Publisher Link]

[20] Zahid A. Bhat et al., "A Compact and Reconfigurable Dual-Mode Configuration Substrate Integrated Waveguide Dual-Band Bandpass Filter for 5G and Millimeter-Wave Communications," *Progress in Electromagnetics Research Letters*, vol. 99, pp. 93-101, 2021. [CrossRef] [Google Scholar] [Publisher Link]

[21] Sukomal Dey et al., "Frequency and Bandwidth Tunable Reliable MEMS Bandpass Filter for 24 GHz Radar Applications," *International Journal of RF and Microwave Computer-Aided Engineering*, vol. 31, no. 6, pp. 1-14, 2021. [CrossRef] [Google Scholar] [Publisher Link]

[22] Guangxu Shen et al., "Ultra-Low-Loss Millimeter-Wave LTCC Bandpass Filters Based on Flexible Design of Lumped and Distributed Circuits," *IEEE Transactions on Circuits and Systems II: Express Briefs*, vol. 68, no. 4, pp. 1123-1127, 2021. [CrossRef] [Google Scholar] [Publisher Link]

[23] Marie Mbeutcha et al., "Replicability of a Millimeter-Wave Microstrip Bandpass Filter using Parallel Coupled Lines," *2018 IEEE MTT-S Latin America Microwave Conference (LAMC 2018)*, Arequipa, Peru, pp. 1-3, 2018. [CrossRef] [Google Scholar] [Publisher Link]

[24] Yu-Chen Lin et al., "Millimeter-Wave Bandpass Filter on Printed Circuit Board with Conventional Microstrip Line Structure," *2021 International Symposium on Antennas and Propagation (ISAP)*, Taipei, Taiwan, pp. 1-2, 2021. [CrossRef] [Google Scholar] [Publisher Link]

[25] Viktor G. Veselago, "The Electrodynamics of Substances with Simultaneously Negative Values ∈ of and μ," *Soviet Physics Success*, vol. 10, no. 4, pp. 509-514, 1968. [CrossRef] [Google Scholar] [Publisher Link]

[26] J.B. Pendry et al., "Magnetism from Conductors and Enhanced Nonlinear Phenomena," *IEEE Transactions on Microwave Theory and Techniques*, vol. 47, no. 11, pp. 2075-2084, 1999. [CrossRef] [Google Scholar] [Publisher Link]

[27] D.R. Smith et al., "Electromagnetic Parameter Retrieval from Inhomogeneous Metamaterials," *Physics Review E*, vol. 71, pp. 1-11, 2005. [CrossRef] [Google Scholar] [Publisher Link]

[28] D.R. Smith et al., "Composite Medium with Simultaneously Negative Permeability and Permittivity," *Physical Review Letters*, vol. 84, pp. 4184-4187, 2000. [CrossRef] [Google Scholar] [Publisher Link]

[29] Seif Naoui, Lassaad Latrach, and Ali Gharsallah, "Equivalent Circuit Model of Double Split Ring Resonators," *International Journal of Microwave and Optical Technology*, vol. 11, no. 1, pp. 1-6, 2016. [Google Scholar] [Publisher Link]

[30] Mukesh Kumar Khandelwal, Binod Kumar Kanaujia, and Sachin Kumar, "Defected Ground Structure: Fundamentals, Analysis, and Applications in Modern Wireless Trends," *International Journal of Antennas and Propagation*, vol. 2017, no. 1, pp. 1-22, 2017. [CrossRef] [Google Scholar] [Publisher Link]